Georg-August-Universität

Göttingen

SPATIAL COUPLING IN AEROELASTICITY BY MESHLESS KERNEL-BASED METHODS

Holger Wendland

Preprint Nr. 2006-18

European Conference on Computational Fluid Dynamics
ECCOMAS CFD 2006
P. Wesseling, E. Oñate and J. Périaux (Eds)

SPATIAL COUPLING IN AEROELASTICITY BY MESHLESS KERNEL-BASED METHODS

Holger Wendland*

*Institut für Numerische und Angewandte Mathematik, Universität Göttingen
Lotzestr. 16-18, D-37083 Göttingen, Germany
e-mail: wendland@math.uni-goettingen.de
web page: http://www.num.math.uni-goettingen.de/wendland

Key words: Fluid-structure interaction, partitioned or staggered algorithm, radial basis function

Abstract. *This paper gives a survey on kernel-based scattered data interpolation methods in the context of static aeroelastic computations. We describe the general procedure, address problems and solutions for large-scale data sets, for flat data sets, and for rotational information. Finally, we demonstrate the versatility of the method by showing two examples.*

1 INTRODUCTION

In computational aeroelasticity, one major goal is to describe the influence of an elastic structural behavior on the aerodynamic load distribution and the impact of aerodynamic forces on structural deformations. Deformations of an aircraft during flight may have severe consequences on the aerodynamic performance, maneuverability, and handling qualities.[10] For this reason, the elasticity of an aircraft has already to be taken into account during the early stages of design and simulation.

A main task in the treatment of coupled aeroelastic systems is the simulation of fluid-structure interaction (*FSI*). Research on FSI in the field of numerical aeroelastic simulation has recently strongly increased.[2,4,7–9,11] An FSI method derives an adequate numerical distribution of aerodynamic loads at the structural nodes of the FE-model - using the aerodynamic pressures given in finite volumes, volume elements, or panels of the discretized flow-field or surface - as well as an adequate deformation of the aerodynamic shape - using the displacements and rotations given at the nodes of the FE-model.

In the literature, there exist two main formulations to describe the aeroelastic problem: the monolithic and the coupled field formulation.[9,14] In the first case, and especially for simple and small-scale structural problems, the fluid and the structural state equations are combined and treated as a single monolithic system of equations. However, for complex aeroelastic problems, the fluid and the structural domains show different mathematical

and numerical properties and require distinct numerical solvers. For the monolithic approach, a rewriting of the structural and fluid computer programs is necessary and the extension to other disciplines is difficult to realize. Consequently, the simultaneous solution by a monolithic scheme is in general computationally challenging, mathematically and economically suboptimal, and software-wise unmanageable.[9]

In the non-monolithic approach, existing well-established numerical solvers can be used. The interaction between the fluid and structural codes is limited to the exchange of surface loads and surface deformation information using partitioned or staggered procedures.[9] This approach allows an easier extension to multidisciplinary problems as they appear, for example, in aerothermoelasticity or aeroservoelasticity.

Usually, the solution of dynamic aeroelastic problems needs a coupling in space and time, whereas in static problems only coupling in space is necessary. For coupling in time partitioned or staggered solution procedures[9] are widely used. For coupling in space recently both, purely mathematically and physically motivated approaches[6,12,13,15] were presented.

Because both, the aerodynamic and structural models are discretized in a physically different manner, they do not match at the boundary. This means, that the models do not share the same grid points at their common boundary. Even more, in many cases both models do not even have a common boundary but only an approximate common boundary. There might be substantial overlap and intersection between both models, or, the structural model is entirely contained within the aerodynamical model of the aircraft.

Consequently, the structural discretization is not useful to model the aerodynamic shape since there are, in general, not enough elements or nodes to represent a sufficiently smooth surface. Hence, the structural model is often smaller than the aerodynamic model by orders of magnitude.

In this paper, we will discuss recent developments using partitioned or staggered algorithms based upon meshless, kernel-based methods, particularly upon interpolation by positive definite and radial basis functions.[1–3]

This paper is organized as follows. In the next section we will shortly outline the FSI problem more precisely. The third section will discuss the coupling procedure and typical physical requirements such as the conservation of discrete work and forces, as well as problems that arise, when rotations have to be recovered or the structural model is actually only two dimensional. The last section gives some results from numerical computations.

2 THREE FIELD FORMULATION

Fluid-structure-interaction problems are generally described in a so called three field formulation, referring to the fluid domain, the structural domain and the interface between both of them.

To be more precise, let $\Omega(t)$ be a time dependent domain of $\mathbb{R}^3$. We will assume that $\overline{\Omega(t)} = \overline{\Omega_F(t)} \cup \overline{\Omega_S(t)}$ for all time and $\Omega_F(t) \cap \Omega_S(t) = \emptyset$. Here, $\Omega_F(t)$ denotes the domain

occupied by the fluid at time t, while $\Omega_S(t)$ denotes the structural domain. Finally, let $\Gamma(t) = \overline{\Omega_F(t)} \cap \overline{\Omega_S(t)}$ be the fluid-structure interface.

On $\Omega_F(t)$ the governing equations that describe the flow are given by the Navier-Stokes or Euler equations. These equations are based on the conservation of mass, momentum, and energy. In our application, we will restrict ourselves to the Euler equations for compressible flow,

$$\begin{aligned} \frac{\partial \rho}{\partial t} + \nabla \cdot (\rho \mathbf{u}) &= 0 && (1) \\ \frac{\partial \mathbf{u}}{\partial t} + \mathbf{u} \cdot \nabla \mathbf{u} + \frac{1}{\rho} \nabla p &= \mathbf{0} && (2) \\ \frac{\partial E}{\partial t} + \nabla \cdot ((E+p)\mathbf{u}) &= 0 && (3) \end{aligned}$$

coming from the conservation of mass (1), momentum (2), and energy (3).

Here, $\mathbf{u}$ denotes the velocity field, p the pressure, ρ the density, and $E = \rho(e + \|\mathbf{x}\|_2^2/2)$ the energy (where e is the internal energy and $\mathbf{x} \in \mathbb{R}^3$ the position vector). Density, pressure, temperature, and internal energy are often functions from each other. Their connection is described by laws from thermodynamics. Details can be found in.[5]

The solution of the Euler equations produces a pressure distribution on the aerodynamical surface of the aircraft, which results into forces. These forces are responsible for the lift of the aircraft. However, for elastic structures these forces lead also to a deformation of (parts) of the structure, which, in realistic computations, cannot be neglected.

These deformations are typically described by the Lamé or Navier-Cauchy equations

$$\rho \ddot{\mathbf{s}} = \mu \Delta \mathbf{s} + (\mu + \lambda) \nabla (\nabla \cdot \mathbf{s}) + \mathbf{b}, \tag{4}$$

where λ and μ are the Lamé constants and represent the elastic properties of the structure, $\mathbf{s}$ is the displacement field, $\mathbf{b}$ are the body and external forces, and ρ is the density of the body.

In particular in aeroelastic computations, an eigen mode formulation of (4) is used. Suppose the displacements $\mathbf{s}$ are expressed as

$$\mathbf{s}(\mathbf{x}, t) = \sum_{n=1}^{\infty} q_n(t) \boldsymbol{\psi}_n(\mathbf{x}),$$

where the functions $\boldsymbol{\psi}_n(\mathbf{x})$ are the natural eigen modes of vibration of the structure and $q_n(t)$ are the Lagrange variables. Then, using only a finite number of Lagrange variables, (4) can be expressed as

$$\sum_{p=1}^{N} M_{np} \ddot{q}_p(t) + \sum_{p=1}^{N} K_{np} q_p(t) = e_n, \qquad 1 \le n \le N, \tag{5}$$

where $M = (M_{np})$ is the mass and $K = (K_{np})$ the stiffness matrix, and e_n results from the body and external forces.

The aerodynamical and the structural mechanical problem both have to be completed by appropriate boundary and initial conditions. In the context of FSI problems (some of) these boundary conditions are given by the other problem. To be more precise, on $\Gamma(t)$ we have to transfer

- forces from the fluid problem, which are integrated pressures, to the structural domain,
- displacements, resulting from the structural solver, to the fluid domain.

Classical partitioned procedures for an FSI problem use classical solvers for the aerodynamical and structural problem. In the first case, a Finite Volume method in an Eulerian description is usually used. In the latter case, Finite Elements in a Lagrangian formulation are the standard method.

3 COUPLING PROCEDURE

Several different coupling procedures have been studied. Amongst them, the most promising are those based on interpolation methods used for transferring displacements from the structural to the aerodynamical mesh. For transferring forces, interpolation should not be used, since it does not reflect the correct physical behavior.

Interpolation by (conditionally) positive definite kernels is one of the most flexible methods allowing to couple arbitrary geometries by reducing them to pure nodal information.

To describe it more precisely, let us introduce the following notation.

- Structural side:
  - $X = \{\mathbf{x}_1, \dots, \mathbf{x}_N\}$ is the set of nodes,
  - $\mathbf{f} = (\mathbf{f}(\mathbf{x}_1), \dots, \mathbf{f}(\mathbf{x}_N))$ are the forces that have to be computed during the coupling process,
  - $\mathbf{g} = (\mathbf{g}(\mathbf{x}_1), \dots, \mathbf{g}(\mathbf{x}_N))$ are the displacements that are given by the structural solver.
- Aerodynamical side:
  - $Y = \{\mathbf{y}_1, \dots, \mathbf{y}_M\}$ is the set of nodes,
  - $\mathbf{F} = (\mathbf{F}(\mathbf{y}_1), \dots, \mathbf{F}(\mathbf{y}_M))$ are the forces that are computed by the fluid solver,
  - $\mathbf{G} = (\mathbf{G}(\mathbf{y}_1), \dots, \mathbf{G}(\mathbf{y}_M))$ are the displacements that have to be computed during the coupling process.

Note that the involved forces and displacements $\mathbf{f}(\mathbf{x}_j), \mathbf{g}(\mathbf{x}_j), \mathbf{F}(\mathbf{y}_j)$, and $\mathbf{G}(\mathbf{y}_j)$ are $3D$ vectors. Hence, from now on $\mathbf{f}_i = (f_i(\mathbf{x}_1), \dots, f_i(\mathbf{x}_N))^T \in \mathbb{R}^N$ denotes the ith component of the Matrix $\mathbf{f}$, and so on.

3.1 Using Interpolation to Exchange Displacements

3.1.1 The General Procedure

A radial basis function interpolant is a function of the form

$$s(\mathbf{x}) = \sum_{j=1}^{N} \alpha_j \Phi(\mathbf{x} - \mathbf{x}_j) + p(\mathbf{x}). \tag{6}$$

Here, $\Phi : \mathbb{R}^3 \to \mathbb{R}$ is a (conditionally) positive definite function of a certain order m and $p \in \pi_{m-1}(\mathbb{R}^3)$ is a 3-variate polynomial of degree at most $m-1$. The coefficient vector $\boldsymbol{\alpha} \in \mathbb{R}^N$ as well as the polynomial p are determined by the interpolation conditions

$$s(\mathbf{x}_j) = v_j, \qquad 1 \le j \le N,$$

where $v_j = g_i(\mathbf{x}_j)$ are the given deformation for the ith coordinate (i between 1 and 3 is from now on considered fixed) together with the additional conditions

$$\sum_{j=1}^{N} \alpha_j q(\mathbf{x}_j) = 0, \qquad \text{for all } q \in \pi_{m-1}(\mathbb{R}^3).$$

In general, linear polynomials are included even for those basis functions, where this would not be necessary by theory, i.e. if basis functions are employed which are conditionally positive definite of order 0 or 1. The reason for this is, that this guarantees that rigid body motions are exactly recovered. Hence, a typical interpolation matrix has the form

$$A = \begin{pmatrix} \Phi(\mathbf{x}_1 - \mathbf{x}_1) & \Phi(\mathbf{x}_1 - \mathbf{x}_2) & \cdots & \Phi(\mathbf{x}_1 - \mathbf{x}_N) & 1 & x_1 & y_1 & z_1 \\ \Phi(\mathbf{x}_2 - \mathbf{x}_1) & \Phi(\mathbf{x}_2 - \mathbf{x}_2) & \cdots & \Phi(\mathbf{x}_2 - \mathbf{x}_N) & 1 & x_2 & y_2 & z_2 \\ \vdots & & & \vdots & & & \vdots & \\ \Phi(\mathbf{x}_N - \mathbf{x}_1) & \Phi(\mathbf{x}_N - \mathbf{x}_2) & \cdots & \Phi(\mathbf{x}_N - \mathbf{x}_N) & 1 & x_N & y_N & z_N \\ 1 & 1 & \cdots & 1 & 0 & 0 & 0 & 0 \\ x_1 & x_2 & \cdots & x_N & 0 & 0 & 0 & 0 \\ y_1 & y_2 & \cdots & y_N & 0 & 0 & 0 & 0 \\ z_1 & z_2 & \cdots & z_N & 0 & 0 & 0 & 0 \end{pmatrix},$$

where we have used the notation $\mathbf{x}_j = (x_j, y_j, z_j)$. The matrix has a typical block structure and can obviously be represented in the form

$$A = \begin{pmatrix} A_{\Phi,X} & P_X \\ P_X^T & 0 \end{pmatrix}. \tag{7}$$

This matrix is, for an appropriate choice of basis function Φ, always invertible if the structural points X are not located on a two dimensional plane.[18]

Introducing in the same way the matrices $A_{\Phi,X,Y} = (\Phi(\mathbf{y}_i - \mathbf{x}_j))$ and $P_Y = (p_j(\mathbf{y}_i))$, it is easy to see that evaluating the interpolant at the aerodynamical nodes defines a coupling matrix $H : \mathbb{R}^N \to \mathbb{R}^M$ via

$$s|Y = \begin{pmatrix} A_{\Phi,X,Y} & P_Y \end{pmatrix} \begin{pmatrix} A_{\Phi,X} & P_X \\ P_X^T & 0 \end{pmatrix}^{-1} \begin{pmatrix} \mathbf{v} \\ 0 \end{pmatrix} =: \begin{pmatrix} H & \widetilde{H} \end{pmatrix} \begin{pmatrix} \mathbf{v} \\ 0 \end{pmatrix}. \tag{8}$$

This coupling matrix maps the x, y, z-components of the displacement vectors on the structural side to the x, y, z-components of the displacement vectors on the aerodynamical side, i.e.

$$\mathbf{G}_i = H\mathbf{g}_i, \qquad 1 \le i \le 3.$$

3.1.2 Speed-up Methods for Large-Scale Data Sets

If the set of structural nodes and/or the set of aerodynamical nodes contains too many points a direct set up of the coupling matrix H is either too time consuming or not even possible. The overall computational cost is given by $\mathcal{O}(N^3 + MN^2)$ for computing the coupling matrix and $\mathcal{O}(MN)$ for each coupling step, the storage requirement is $\mathcal{O}(MN)$. For high resolution, large-scale models, where the structure can consist of several tenth thousand points and the aerodynamical aircraft model of several million points, this is beyond the capacity of standard computers. Hence, fast evaluation methods have to be employed. For interpolation by radial basis functions such fast evaluation methods are well-known and well investigated. They are either based upon a compactly supported RBF, or a far or near field expansion of the kernel, or a partition of unity approach. More details can be found in[18] and the literature given therein.

The method of our choice is the partition of unity method, where the computational domain is subdivided into several smaller regions. On each such region the interpolation problem is solved locally and the local interpolants are glued together by a partition of unity family. Details can be found in.[3, 17]

In any case, such methods allow us to reduce the complexity to linear $\mathcal{O}(N)$ complexity for computing the interpolant and constant complexity for each evaluation, i.e. $\mathcal{O}(M)$ complexity for each coupling step. Such a reduced complexity is crucial when it comes to coupling also in time.

3.1.3 Dealing with Rotations

In contrast to high-resolution models, one also often finds very reduced structural models. The best known case is the structural grid of the AMP test wing, which is sometimes reduced to a simple rod, see Figure 1.

For such reduced models, often not only displacement vectors at the nodes are known but also rotational information is given. In our terminology, this means that for each $\mathbf{x}_j$

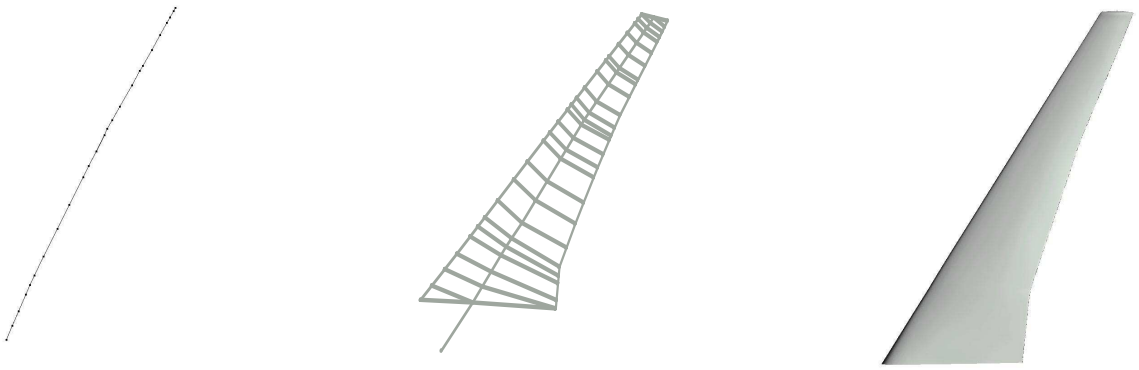

Figure 1: Two structural models (left and middle) and the aerodynamical model (right) of the AMP wing

we are given not only the displacements $\mathbf{g}(\mathbf{x}_j)$ but also angles $\boldsymbol{\theta}_j \in \mathbb{R}^3$. Since (small) angles can be related to derivatives of the displacement field via

$$\begin{pmatrix} \theta_x \\ \theta_y \\ \theta_z \end{pmatrix} = \frac{1}{2} \begin{pmatrix} 0 & -\frac{\partial}{\partial z} & \frac{\partial}{\partial y} \\ \frac{\partial}{\partial z} & 0 & -\frac{\partial}{\partial x} \\ -\frac{\partial}{\partial y} & \frac{\partial}{\partial x} & 0 \end{pmatrix} \begin{pmatrix} g_1 \\ g_2 \\ g_3 \end{pmatrix} =: \frac{1}{2} \nabla \times \mathbf{g},$$

we are now looking for an interpolant $\mathbf{s} : \mathbb{R}^3 \to \mathbb{R}^3$ satisfying

$$\mathbf{s}(\mathbf{x}_i) = \mathbf{g}(\mathbf{x}_i), \qquad \nabla \times \mathbf{s}(\mathbf{x}_i) = 2\boldsymbol{\theta}(\mathbf{x}_i), \qquad 1 \leq i \leq N.$$

Recently,[1] a modification of (6) has been proposed to meet these generalized interpolation conditions. Note that this time the three components of the displacement field cannot be recovered independently. The suggested modification consists of replacing the kernel $\Phi : \mathbb{R}^3 \to \mathbb{R}$ by a matrix-valued function $\Phi : \mathbb{R}^3 \to \mathbb{R}^{3\times 3}$ and the coefficients $\alpha_j \in \mathbb{R}$ by vectors $\boldsymbol{\alpha}_j \in \mathbb{R}^3$. Moreover, to achieve a symmetric interpolation matrix again, the data giving functionals have to be incorporated into the interpolant. To be more precise (6) has to be replaced by

$$\mathbf{s}(\mathbf{x}) := \sum_{j=1}^{N} \Phi(\mathbf{x} - \mathbf{x}_j)\boldsymbol{\alpha}_j + \sum_{j=1}^{N} (\delta_{\mathbf{x}_j} \circ (\mathrm{curl}))^{\mathbf{y}} \Phi(\mathbf{x} - \mathbf{y})\boldsymbol{\alpha}_{N+j}, \tag{9}$$

which can also be enriched by (vector-valued) polynomials. Here, the superscript $\mathbf{y}$ denotes the fact that the functional acts with respect to the second variable of the kernel and $\delta_{\mathbf{x}_j}$ denotes point evaluation at $\mathbf{x}_j$. More details on this approach can be found in.[1]

3.1.4 Dealing with Flat Structural Points

The AMP test wing is also an example for a a structural model, which is actually only two dimensional, while the aerodynamical model is three dimensional. This means that

we have deformations only on a two dimensional subset but need to transfer them to a three dimensional model. Such an extrapolation problem is always problematic concerning reliability. Moreover, the classical coupling matrix (7) will be singular in such a situation. Nonetheless, the problem of finding the coefficient vectors of the interpolant (6) is still solvable, since the right hand side of

$$A \begin{pmatrix} \boldsymbol{\alpha} \\ \boldsymbol{\beta} \end{pmatrix} = \begin{pmatrix} \mathbf{v} \\ \mathbf{0} \end{pmatrix}$$

belongs to the image of the matrix A. Hence, a solution to this linear problem exists, though it is not unique. It can, for example, be computed using a singular value decomposition or a QR decomposition of the coefficient matrix A. Another possibility of avoiding singularity of the matrix A is to use only two dimensional polynomials. This can be justified as follows. Suppose the structural points are located on a plane, which is given by two orthogonal unit vectors $\mathbf{r}$ and $\mathbf{t}$ and an additional vector $\mathbf{a}$, such that each point $\mathbf{x}$ on the plane has a representation

$$\mathbf{x} = \mathbf{a} + \mu\mathbf{r} + \nu\mathbf{t}$$

with two parameters $\mu, \nu \in \mathbb{R}$. Denoting the parameters for $\mathbf{x}_j$ by $\boldsymbol{\mu}_j = (\mu_j, \nu_j)$, we see that

$$\|\mathbf{x}_i - \mathbf{x}_j\|_2 = \|\boldsymbol{\mu}_i - \boldsymbol{\mu}_j\|_2.$$

Moreover, the polynomial part of the interpolant (6), given by

$$p(\mathbf{x}) = \beta_0 + \beta_1 x + \beta_2 y + \beta_3 z$$

has the representation

$$p(\mathbf{x}) = \beta_0 + \boldsymbol{\beta}^T\mathbf{a} + (\boldsymbol{\beta}^T\mathbf{r})\mu_j + (\boldsymbol{\beta}^T\mathbf{t})\nu_j =: \gamma_0 + \gamma_1\mu_j + \gamma_2\nu_j,$$

where we have set $\boldsymbol{\beta} = (\beta_1, \beta_2, \beta_3)$. Hence, the interpolant (6) can entirely be written as a function of the two dimensional points $\boldsymbol{\mu}_j$. Since the $\boldsymbol{\mu}_j$ have to be pairwise distinct themselves, and are hopefully not located on a line (otherwise we have actually to repeat the procedure just described to derive a one dimensional problem), we are now in the situation of an invertible matrix.

3.2 Exchanging Forces

Whenever the exchanging of displacements is reduced to nodal information, the exchange process can be described by a coupling matrix $H : \mathbb{R}^N \to \mathbb{R}^M$ if the components are handled independently or by a coupling matrix $H : \mathbb{R}^{3N} \to \mathbb{R}^{3M}$ otherwise.

In both cases, the coupling matrix can be used to transfer forces from the aerodynamical to the structural grid via

$$\mathbf{f}_i = H^T\mathbf{F}_i, \qquad 1 \le i \le 3.$$

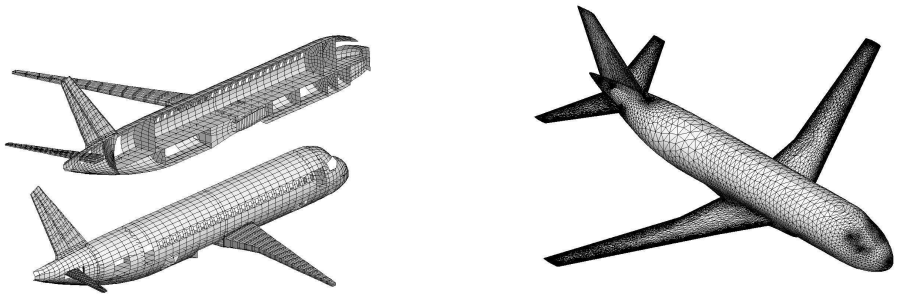

ht

Figure 2: Structural and aerodynamic model of Alenia's SMJ Model

(or $\mathbf{f} = H^T\mathbf{F}$ in the non-independent case, which we will not address further on). It is important to see that this definition of exchanging forces already guarantees the conservation of discrete work, since

$$\sum_{j=1}^{N} f_i(\mathbf{x}_j)g_i(\mathbf{x}_j) = \mathbf{f}_i^T\mathbf{g}_i = (H^T\mathbf{F}_i)^T\mathbf{g}_i = \mathbf{F}_i^T H\mathbf{g}_i = \mathbf{F}_i^T\mathbf{G}_i = \sum_{j=1}^{M} F_i(\mathbf{y}_j)G_i(\mathbf{y}_j)$$

for $1 \leq i \leq 3$.

To conserve also the sum of forces, the coupling matrix needs to be *conservative* in the following sense. If $\mathbf{e}_k$ denotes the vector $\mathbf{e}_k = (1, \ldots, 1)^T \in \mathbb{R}^k$, then H has to satisfy $H\mathbf{e}_N = \mathbf{e}_M$.

If H is conservative in this sense, it immediately follows that

$$\sum_{j=1}^{N} f_i(\mathbf{x}_j) = \mathbf{f}_i^T\mathbf{e}_N = (H^T\mathbf{F}_i)^T\mathbf{e}_N = \mathbf{F}_i^T H\mathbf{e}_N = \mathbf{F}_i^T\mathbf{e}_M = \sum_{j=1}^{M} F_i(\mathbf{y}_j)$$

for $1 \leq i \leq 3$.

4 EXAMPLES

4.1 Alenia's SMJ Model

Interpolation by radial basis functions as the coupling procedure in Aeroelasticity has intensively been studied. Here, we present some details of a test computation performed on Alenia's SMJ aircraft, see Figure 2. A more thorough presentation of the results can be found in.[3]

Table 1 shows the differences between an aeroelastic and a rigid computation.

The deformation of the structure (see Figure 3, left) leads to a decrease of the total lift as shown in Figure 3. Beside this decreased lift, a different behavior of the span-wise C_p distribution at the wing tip is given.

	elastic	rigid	$\Delta\%$
Lift C_l	0.431	0.508	-15
Drag C_d	0.0299	0.0368	-18

Table 1: Influence of elasticity

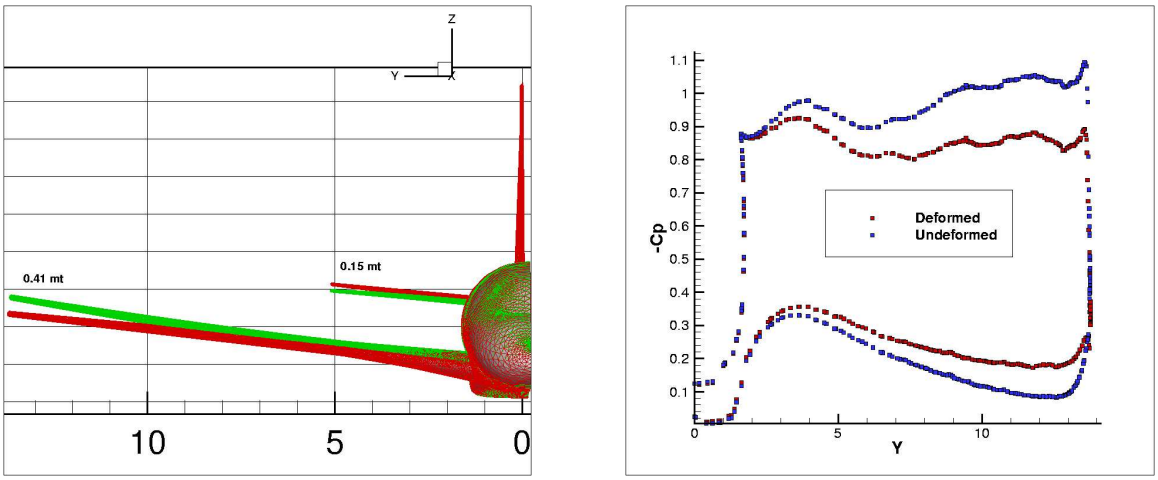

Figure 3: Deflection and Pressure Distribution

This phenomenon can be explained by a vortex at the trailing edge of the wing tip. In this region, the fluid particles undergo a rapid acceleration when passing the tip and produce a local vortex that increases the Mach number to a maximum value of 1.4. Table 1 summarizes the differences between the elastic and rigid computations in terms of lift and drag. Clearly, the influence of the elasticity cannot be neglected.

4.2 Recovery of Rotations

Our second example deals with the reconstruction of rotations for the AMP test wing, shown in Figure 1. For testing purposes, we applied the following simple, analytic displacements to the structural grid:

$$\mathbf{g}(\mathbf{x}) = \left(0, 0, 0.1y^2 + 0.1x\right)^T.$$

Then, the displacements were carried over to the fluid grid by standard interpolation (6) and by the vector-valued interpolant (9) incorporating also the fact that this displacement field induces a rotation of the form

$$\boldsymbol{\theta} = \nabla \times \mathbf{g}(\mathbf{x}) = (0.2y, -0.1, 0)^T.$$

In both cases, we used the same radial basis function, the compactly supported C^2 Wendland function[16] $\Phi(\mathbf{x}) = \Phi_\delta(\mathbf{x}) = \phi(\|\mathbf{x}\|_2/\delta)$ with $\phi(r) = (1-r)_+^4(4r+1)$ and with support

radius $\delta = 1.051603$, which corresponds to the longest side of the bounding box of the structural model. Furthermore, we included linear polynomials.

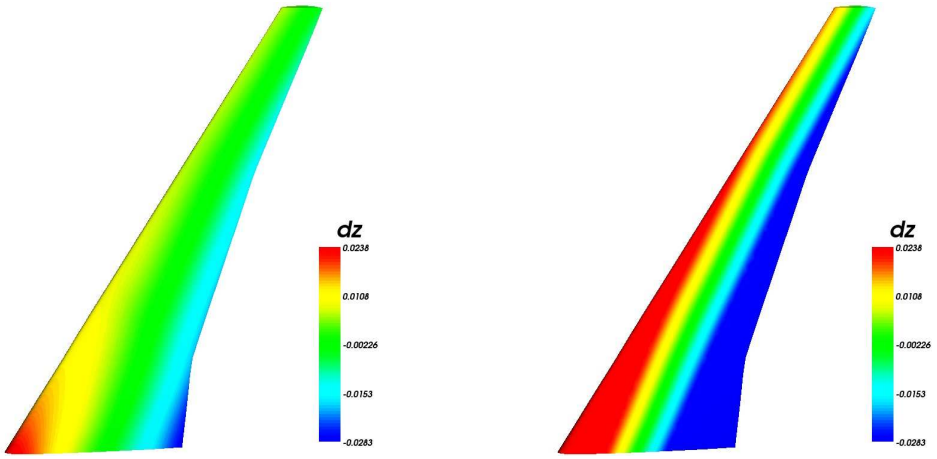

Figure 4: Results for the AMP test wing with (left) and without (right) the reconstruction of rotations

Figure 4 shows the error for both methods on the aerodynamic side. Clearly, in both cases the error is the largest close to the root of the wing, where structural and aerodynamic meshes differ most. But it is also apparent that the generalized interpolant (9) is much more capable of recovering the deformations caused by rotation at the leading and trailing edge of the aerodynamic model.

REFERENCES

[1] R. Ahrem, A. Beckert, and H. Wendland. Recovering rotations in spatial coupling for fluid-structure-interaction problems. Preprint, Göttingen 2005.

[2] R. Ahrem, A. Beckert, and H. Wendland. A new multivariate interpolation method for large-scale spatial coupling problems in aeroelasticity. In *Conference Proceedings to the Int. Forum on Aeroelasticity and Structural Dynamics (IFASD)*, DGLR-Bericht 2005-04. DGLR, 2005.

[3] R. Ahrem, A. Beckert, and H. Wendland. A meshless spatial coupling scheme for large-scale fluid-structure-interaction problems. *Computer Modeling in Engineering & Sciences*, 12:121–136, 2006.

[4] A. Beckert and H. Wendland. Multivariate interpolation for fluid-structure-interaction problems using radial basis functions. *Aerosp. Sci. Technol.*, 5:125–134, 2001.

[5] R. L. Bisplinghoff and H. Ashley. *Principles of Aeroelasticity*. John Wiley & Sons, Inc., New York, 1962.

[6] J. R. Cebral and R. Löhner. Conservative load projection and tracking for fluid-structure problems. *AIAA Journal*, 35:687–692, 1997.

[7] J. W. Edward. Computational aeroelasticity. In *Flight-Vehicles, Materials, Structures and Dynamics – Assessment and Future Directions*, volume 5. The American Society of Mechanical Engineers, New York, 1993.

[8] C. Farhat, C. Degand, B. Koobus, and M. Lesoinne. An improved method of spring analogy for dynamic unstructured fluid meshes. In *AIAA 98-2070, 39th AIAA/ASME/ASCE/AHS Structures, Structural Dynamics and Materials Conference*, Long Beach, California, 1998.

[9] C. Farhat and M. Lesoinne. Higher-order staggered and subiteration free algorithms for coupled dynamic aeroelasticity problems. In *36th Aerospace Sciences Meeting and Exhibit,AIAA 98-0516, Reno/NV*, 1998.

[10] H. Försching. *Grundlagen der Aeroelastik*. Springer, Heidelberg-Berlin-New York, 1974.

[11] H. Försching. New ultra high capacity aircraft (uhca) - challenges and problems from an aeroelastic point of view. *ZFW*, 18:219–231, 1994.

[12] R. L. Harder and R. N. Desmarais. Interpolation using surface splines. *Journal of Aircraft*, 9:189–197, 1972.

[13] M. H. L. Hounjet and J. J. Meijer. Evaluation of elastomechanical and aerodynamic data transfer methods for non-planar configurations in computational aeroelastic analysis. Technical report, ICAS-Publication, 1994.

[14] P. Kutler. Multidisciplinary computational aerosciences. In *Sendai, Proc. of the 5th Int. Symp. on Comp. Fluid Dynamics*, pages 109–119, 1993.

[15] N. Maman and C. Farhat. Matching fluid and structure meshes for aeroelastic computations: A parallel approach. *Computers and Structures*, 54:779–785, 1995.

[16] H. Wendland. Piecewise polynomial, positive definite and compactly supported radial functions of minimal degree. *Adv. Comput. Math.*, 4:389–396, 1995.

[17] H. Wendland. Fast evaluation of radial basis functions: Methods based on partition of unity. In C. K. Chui, L. L. Schumaker, and J. Stöckler, editors, *Approximation Theory X: Wavelets, Splines, and Applications*, pages 473–483, Nashville, 2002. Vanderbilt University Press.

[18] H. Wendland. *Scattered Data Approximation*. Cambridge Monographs on Applied and Computational Mathematics. Cambridge University Press, Cambridge, UK, 2005.

Institut für Numerische und Angewandte Mathematik
Universität Göttingen
Lotzestr. 16-18
D - 37083 Göttingen

Telefon: 0551/394512
Telefax: 0551/393944

Email: trapp@math.uni-goettingen.de URL: http://www.num.math.uni-goettingen.de

Verzeichnis der erschienenen Preprints:

2006-01	R. Schaback	Limit Problems for Interpolation by Analytic Radial Basis Function
2006-02	N. Bissantz, T. Hohage, A. Munk, F. Ruymgaart	Convergence rates of general regularization methods for statistical inverse problems and applications
2006-03	J. Brimberg, H. Juel, A. Schöbel	Locating a circle on a sphere
2006-04	J. Brimberg, H. Juel, A. Schöbel	Locating a circle on the plane using the minimax criterion
2006-05	L. Ling, R. Opfer, R. Schaback	Results on Meshless Collocation Techniques
2006-06	G. Lube, T. Knopp et.al.	Domain decomposition methods for indoor air flow simulation
2006-07	T. Apel, T. Knopp, G. Lube	Stabilized finite element methods with anisotropic mesh refinement for the Oseen problem
2006-08	R. Schaback	Recovery of Functions From Weak Data Using Unsymmetric Meshless Kernel-Based Methods
2006-09	H.W. Hannacher, S. Horn, A. Schbel	Stop Location Design in Public Transportation Networks: Covering and Accessibility Objective
2006-10	Q.T. Le Gia, F.J. Narcowich, J.D. Ward, H. Wendland	Continuous and Discrete Least-Squares Approximation by Radial Basis Functions on Spheres
2006-11	R. Schaback	Unsymmetric Meshless Methods for Operator Equations

2006-12	P. Giesl, H. Wendland	Meshless Collocation: Error Estimates with Application to Dynamical Systems
2006-13	H. Wendland	On the stability of meshless symmetric collocation for boundary value problems
2006-14	G. Lube	Stabilized FEM for incompressible flow. Critical review and new trends
2006-15	J. Puerto, A. Schöbel, S. Schwarze	A Class of Infinite Potential Games
2006-16	S. Hein, T. Hohage, W. Koch, J. Schöberl	Acoustic Resonances in High Lift Configuration
2006-17	T. Hohage, M.L. Rapún, F.J. Sayas	Detecting corrosion using thermal measurements
2006-18	H. Wendland	Spatial coupling in aeroelasticity by meshless kernel-based methods